JOURNAL OF Applied Polymer SCIENCE

Maleic Anhydride-*grafted*-Polybutadiene as a Controlled Defibrillating and Dispersing Agent for Short Aramid Fiber Reinforced Thermoplastic Polyurethane Composite with Improved Mechanical Properties

G. S. Shibulal, Kinsuk Naskar
Rubber Technology Centre, Indian Institute of Technology, Kharagpur 721302, West Bengal, India
Correspondence to: K. Naskar (E-mail: knaskar@rtc.iitkgp.ernet.in)

ABSTRACT: The reinforcing effect of resorcinol formaldehyde latex (RFL) coated short aramid fiber on an ester-based thermoplastic polyurethane (TPU) was investigated on the basis of mechanical properties. Short fibers having different fiber length were used for the reinforcement. The exceptionally high Young's modulus and low strain modulus indicate the reinforcing effect of this fiber on to the TPU matrix. It has been observed that fibers of 3 mm length at 10 phr loading and 6 mm length even at a loading of 5 phr start to exhibit severe fibrillation: the longitudinal splitting of fiber having larger diameter into thinner fibrils during processing. Fibrillation favorably affects the mechanical bonding with the matrix because of the large surface area as well as surface irregularities provided by the fibrillated fiber. However, fibrillation adversely affects the fiber dispersion by enhancing the fiber aggregation. This leads to a greater disturbance in the strain hardening behavior of the TPU matrix and subsequently reducing the tensile strength and elongation at break especially at high fiber loading. Therefore, to control the degree of fibrillation a pre-treatment has been applied on the aramid fiber surface with maleic anhydride-*grafted*-polybutadiene (PB-*g*-MA) prior to mixing it with the TPU matrix. A good quality of fiber dispersion with improved tensile strength and elongation at break has been achieved even with 6 mm short fiber at a loading of 10 phr with the treatment of only 5 phr of PB-*g*-MA. The tensile fractured surface morphological analyses of PB-*g*-MA coated fiber filled TPU composite strongly advocate these results. © 2013 Wiley Periodicals, Inc. J. Appl. Polym. Sci. 130: 2205–2216, 2013

KEYWORDS: polyurethanes; fibers; grafting; morphology; composites

Received 17 February 2013; accepted 9 April 2013; Published online 20 May 2013
DOI: 10.1002/app.39395

INTRODUCTION

Short fibers have gained a remarkable position as reinforcing agent for elastomers, plastics, and thermoplastic elastomers because of its ever-increasing applications in engineering and consumer goods. It offers high strength to weight ratio, high low strain modulus together with good mechanical and thermal properties in comparison with particulate fillers. Moreover, short fiber reinforced polymers offer greater design flexibility compared to continuous fiber filled polymer composites.[1–4] As far as the short fiber reinforcement of polymers is concerned with an aim of improving both mechanical and thermal stability of polar polymers like thermoplastic polyurethane, aramid fiber is one of the potential candidates. These fibers have unique combination of strength, stiffness, and thermal stability.[5] Earlier many researchers have reported various studies carried out with different kinds of aramid short fibers on different types of thermoplastic elastomers (TPEs). For instance, Arroyo et al.[6] reported the morphology/behavior and recyclability of the Twaron® fiber reinforced PP/EPDM TPE. Kutty and Nando[7–9] extensively studied various aspects of Kevlar® short fiber reinforced polyurethane based thermoplastic elastomer. Correa et al.[10,11] have investigated the mechanical and thermal degradation properties of short Twaron fiber reinforced thermoplastic polyurethane. Among the various types of aramid fibers available for the reinforcement, Technora® fibers have found considerable attention in the recent past.[12] Technora® is basically copoly-(paraphenylene-3,4′-oxydiphenylene) terephthalamide. It offers a balance of advantages between meta and para aramid by exhibiting a molecular structure which has both meta and para linkages as shown in Figure 1. It is having high flexibility compared to para and higher tensile strength than its meta variety. Chanthipa et al.[13] have studied the reinforcing effect of this fiber on the mechanical and dynamic mechanical properties of thermoplastic polyurethane as a function of fiber loading and compared the properties with a meta aramid (Conex) reinforced thermoplastic polyurethane (TPU) composite. They have found that both the low strain modulus and the storage modulus of the Technora®/TPU composite were significantly higher than those of the Conex–TPU composites.

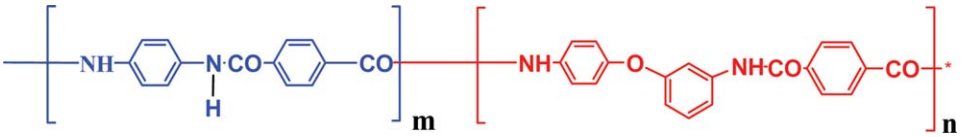

Figure 1. Chemical structure of aramid short fiber (Technora®): co-poly-(paraphenylene/3,4′-oxydiphenylene terephthalamide). [Color figure can be viewed in the online issue, which is available at wileyonlinelibrary.com.]

It is very well documented in the literature that a good quality of fiber dispersion and a high level of interfacial adhesion between the fiber and the matrix are pre-requisite criteria to impart integrated mechanical properties to any short fiber reinforced polymer composite. As far as aramid fiber is concerned, it is very poor in terms of fiber dispersion and the interfacial adhesion between the fiber and the polymer matrix owing to its chemical inertness, high crystallinity, inter-hydrogen bonding, and smooth fiber surface. Therefore, many kinds of surface modifications have been conducted by various researchers to improve its adhesion to the polymer matrix. For instance, Limcharon et al.[14] performed *N*-alkylation on a poly(*m*-phenylene isophthalamide)–Teijin–Conex fiber and studied its interfacial adhesion on thermoplastic elastomer (SEBS). Andreopoulos et al.[15] have studied the surface treatment of aramid fibers by immersion in a solution of methacryloyl chloride in CCl_4 and reported an enhanced flexural properties of such treated fiber reinforced epoxy composite. Very recently Liu et al.[16] have reported that interfacial strength of a Twaron aramid fiber reinforced epoxy composite was enhanced by about 50% after modifying the fiber surface with epoxy chloropropane via Friedel–Craft reaction. Various other methods, such as plasma treatment, incorporation of coupling agent, such as maleic anhydride grafted polymer with a nonpolar part having a structure similar to the polymer matrix were also used to bring fiber–matrix interaction in aramid short fiber reinforced polymers by various researchers.[17–20] The improved fiber adhesion by the use of various thermosetting resins such as resorcinol formaldehyde (RF) and phenol formaldehyde (PF), etc. are also reported.[21] The RF resin is generally used in combination with natural rubber (NR) latex or vinyl pyridine (VP) latex called the resorcinol formaldehyde latex (RFL). The resorcinol formaldehyde component promotes adhesion to the fiber via polar or covalent interaction, while the dried latex co-vulcanizes with the rubber matrix ensuring adhesion to that matrix. For aramid fibers, simple treatment with RFL leads to rubber composite exhibiting low fiber to matrix adhesion with failure often occurring at the fiber–RFL dip interface. This is due to the physical structure of the aramid, which being highly crystalline provides an uninviting surface to the components making up the RFL. Excellent aramid to rubber adhesion can be achieved by first activating the aramid with low molecular weight and highly reactive epoxies prior to RFL treatment.

In this article, the mechanical properties of an RFL coated Technora aramid short fiber reinforced thermoplastic polyurethane was studied as a function of fiber loading and length. The potential use of PB-*g*-MA as a dispersing as well as a controlled defibrillating agent for RFL coated aramid fiber was also explored on the basis of mechanical and morphological analyses.

EXPERIMENTAL

Materials

Thermoplastic Polyurethane, Desmophan 385 E, composed of 4,4′-diphenylmethane diisocyanate hard segment and polyester based soft segment. The melting temperature is around 170°C (obtained from differential scanning calorimetry), density is 1.2 g/cm^3 with a Shore-A hardness of 85 and was obtained from Bayer Chemicals, India. Aramid short fiber (trade name Technora®) with a chemical name copoly-(paraphenylene/3,4′-oxydiphenylene terephthalamide) was obtained from Teijin Aramid BV, The Netherlands. The detail specifications of the fiber are given in Table I. Maleic anhydride adducted 1,2-polybutadiene (trade name Ricon® 131 MA5) having a number average molecular weight (M_n) of 5300, a specific gravity of 0.9 g/cc and maleic anhydride content of 5% was obtained from Sartomer Company.

Preparation of Composites

Formulations used for the preparation of the composites are given in Table II. The short fiber loading was varied from 1 to 10 phr (parts per hundred resin). All the composites were prepared by melt mixing of the components in a Haake Rheomix 600 OS internal mixer having a chamber volume of 85 cm^3 at a temperature of 180°C with a rotor speed of 80 rpm for 8 min. In order to achieve better dispersion, half portion of the polymer was first melted for 1.5 min and to this the short fiber was added and the mixing was continued for another 1 min. The mixing was continued up to 8 min after adding remaining portion of the fiber at 2.5 min at a constant rotor speed of 80 rpm. The modifier (PB-*g*-MA) was incorporated by first warming the modifier at 70–80°C and then added dropwise to the short fiber

Table I. Technical Specifications of RFL Coated Aramid Short Fiber

Parameter/Properties	Value
Color	Gold
Specific gravity (g/cc)	1.39
Equilibrium moisture regain (%)	2
Average fiber length (mm)	1/3/6
Diameter (μm)	10–12
Average aspect ratio (L/D ratio)	91/275/550
Young's modulus (GPa)	20–21
Tensile strength (MPa)	3000–3500
Elongation at break (%)	5–7

Table II. Formulations of the Mixes in phr (Parts Per Hundred Rubber)

Sample designation	Short fiber length (mm)	Short fiber loadings (phr)	PB-*g*-MA (phr)
$1RAF_3$	1	3	-
$1RAF_5$	1	5	-
$1RAF_{10}$	1	10	-
$3RAF_3$	3	3	-
$3RAF_5$	3	5	-
$3RAF_{10}$	3	10	-
$6RAF_3$	6	3	-
$6RAF_5$	6	5	-
$6RAF_{10}$	6	10	-
$3RAF_{10}$ C_3	3	10	3
$3RAF_{10}$ C_5	3	10	5
$3RAF_{10}$ C_{10}	3	10	10
$6RAF_{10}$ C_5	6	10	5

*RAF indicates RFL coated aramid fiber, left side Arabic number indicate fiber length in mm and the subscript indicates its concentration in phr, C stands for the coupling agent (PB-*g*-MA) and the subscript indicates its concentration in phr.

taken in a flask and stirred with a magnetic stirrer at 100°C for 10 min. The modifier/fiber mix is then added into the mixing chamber containing the molten polymer as per the above-mentioned mixing schedule and continued the mixing up to 8 min at the same rpm. After the mixing is over, the composite was discharged and passed through a two roll mill at tight nip once to get maximum orientations of the fibers in the mill direction. The sheet was then pressed in a compression molding press (Moore Press, Birmingham, UK) at 190°C for 3 min at a pressure of 7 MPa and then cooled down to room temperature under the same pressure by circulating cold water.

Characterization of the Composites

Mechanical Properties. The dumb-bell shaped specimens of the composites in parallel and perpendicular directions with respect to the mill direction used for testing were die cut from the compression molded sheet and the testing was done after 24 h of maturation at room temperature. Tensile properties were measured according to ASTM D 412-98A using a universal testing machine Hounsfield H10KS (UK) at a constant cross-head speed of 500 mm/min. All the values were averages of three measurements.

Fiber Breakage Analyses. In order to determine the fiber length distribution after mixing, fibers were extracted from the composite mixture by dissolving out the TPU by using tetrahydrofuran (THF). The extracted fibers were disposed on a glass slide and the images were captured using an optical microscope (OM; Leica DMLM, Germany) with a magnification of 5×.

Morphological Analyses. Tensile fractured samples of the composites were analyzed using a JEOL (JSM 5800, Japan) scanning electron microscope (SEM). The samples were sputter coated with gold prior to the analyses.

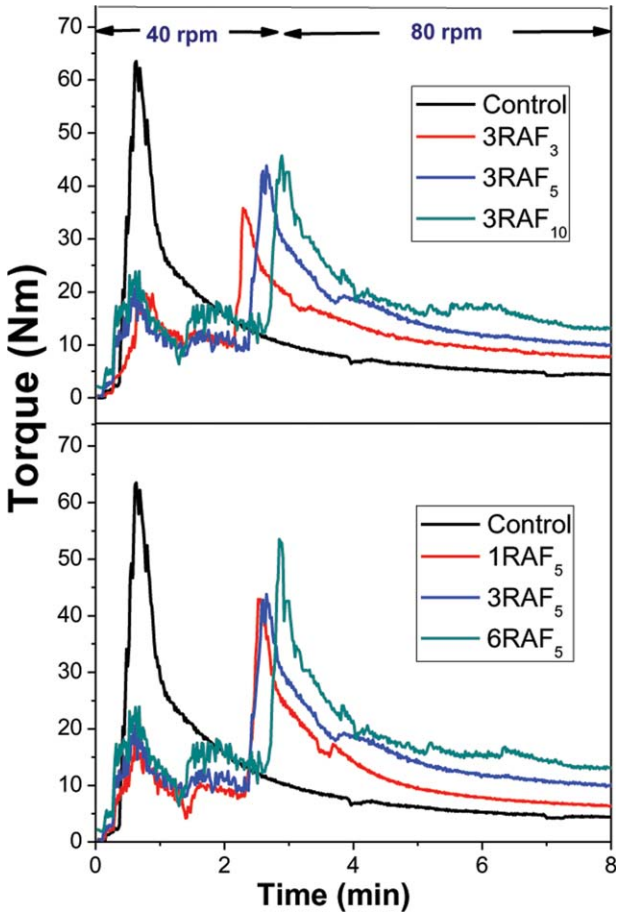

Figure 2. Mixing torque–time curves of TPU/short fiber composite as a function of fiber loading and length. [Color figure can be viewed in the online issue, which is available at wileyonlinelibrary.com.]

RESULTS AND DISCUSSION

The Mixing Characteristics: Effect of Short Fiber Length and Loading

The mixing torque–time relationship of the TPU/short fiber composite as a function of fiber loading and length is shown in Figure 2 and Table III. The torque–time curves show high initial torque with irregular broad peaks between 0 and 3 min, which is due to the sequential feeding of the polymer in the pellet

Table III. Mixing Characteristics of TPU/Short Fiber Composites in Haake Rheomix

Mix code	Torque at 8th minute (Nm)	Delta torque (Nm)	Melt temperature at dumping (°C)
Control	4.5	-	188.0
$3RAF_3$	7.1	2.6	195.0
$3RAF_5$	9.2	4.7	200.8
$3RAF_{10}$	11.2	6.7	202.0
$1RAF_5$	6.0	1.5	198.6
$6RAF_5$	11.2	7.2	204.3

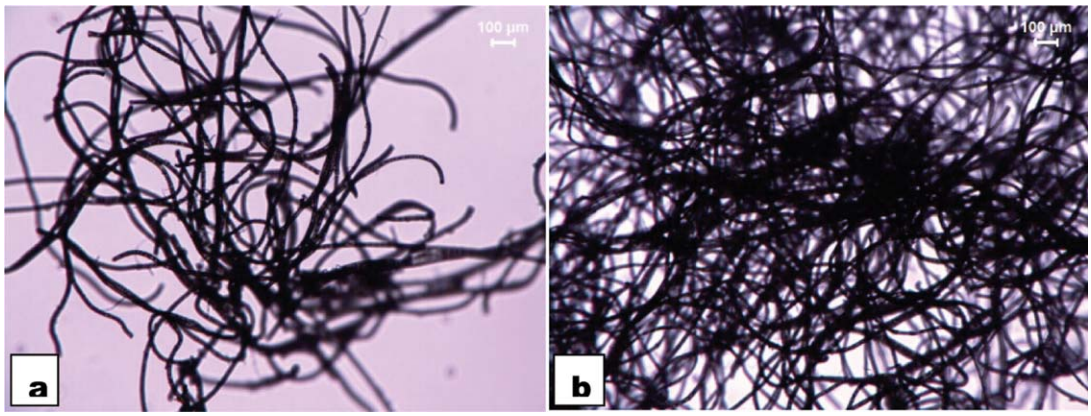

Figure 3. Optical micrographs of short fibers extracted from composites (a) $3RAF_{10}$ and (b) $6RAF_{10}$ (scale bar is 100 μm). [Color figure can be viewed in the online issue, which is available at wileyonlinelibrary.com.]

form followed by the incorporation of dry fiber. As per the mixing sequence, the ram has to be opened at the end of 1.5 and 2.5 min of mixing. Since the torque sensing is a continuous process throughout the mixing cycle, it shows a lower torque at these points. The mixing torque starts to reduce beyond third minute and shows a plateau region of nearly constant mixing torque after all the mixing sequence is over. The stabilized torque value of the composite and the stock temperature were found to increase with an increase in both short fiber loading and length. The torque is seen to increase progressively to approximately 150% of pure TPU when 10 phr of 3 mm short fiber is added to the TPU melt. At a constant loading of 5 phr for 1, 3, and 6 mm short fibers on TPU, the percentage rise of torque with respect to the pure TPU were 33, 104, and 160%, respectively. This effect can be explained with the change in melt viscosity of the polymer fiber composite as a result of fiber addition. Fibers, when added into TPU melt tend to perturb its normal flow by hindering the mobility of chain segments in flow.[22] This leads to a higher melt viscosity than the pure polymer. Increasing the fiber loading and length further restrict the melt flow, which leads to an increased viscosity of the TPU/short fiber suspension. Since viscosity is directly related to torque (at constant temperature and rotor speed), it requires higher torque for mixing. The increase in the melt temperature with increase in short fiber loading and length can be originated from frictioning between the fiber and the polymer and in between fibers during the shear mixing.

Fiber Breakage Analyses

Fibers usually undergo breakage due to the high shear force developed during mixing. Composites $3RAF_{10}$ and $6RAF_{10}$ were used to measure the extent of fiber breakage during processing. The OM images of the extracted fibers from the above mentioned composite mixes are shown in Figure 3(a,b). Usually the extracted fibers are individually deposited on a glass plate and then capturing the OM images. Here we could not separate the fibers individually and whatever the fibers got separated exist in a highly coiled state making it difficult to measure the actual fiber length. This may be due to fibrillation or due to the better retention of the original fiber length owing to the flexible nature of the Technora Aramid short fiber. Drastic fiber breakage has been reported in TPU composite with Kevlar and Twaron Aramid short fibers under the same processing conditions.[7,23]

Mechanical Properties of the Composites as a Function of Fiber Length and Loading

Stress–Strain Behavior. It has been established that thermoplastic polyurethanes are randomly segmented copolymers composed of hard and soft segments forming a two phase microstructure because of the intrinsic incompatibility between the two. Generally, the hard domains are immersed in soft rubbery segments. Some of the earlier studies on the segmental (hard and soft) orientation of TPU during the tensile deformation have been revealed that the strain induced crystallization of soft segment is accomplished in the direction of tensile stress within 200%. Even greater strain induced crystallization in TPU has been observed beyond 500% of strain due to the alignment of hard domains to the applied strain.[24,25] The stress–strain behavior of the neat TPU used in the present investigation with a schematic representation of the orientations of the soft and hard segments within 200–300% of strain and a strain greater than 500% is shown in Figure 4. The stress–strain behavior of

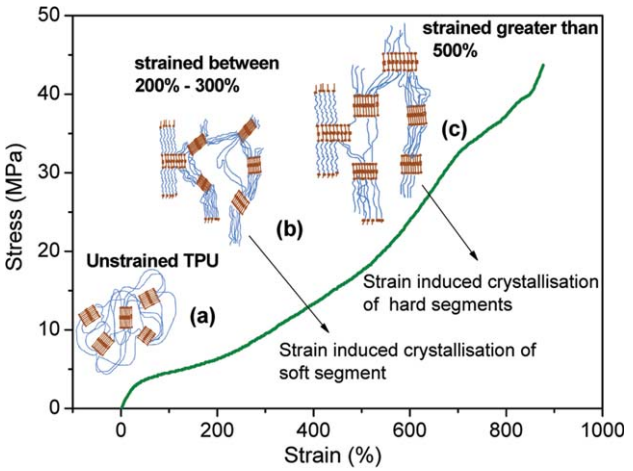

Figure 4. Stress–strain behavior of neat TPU with schematic representations of the plausible orientations of soft and hard segments under various strain ranges. [Color figure can be viewed in the online issue, which is available at wileyonlinelibrary.com.]

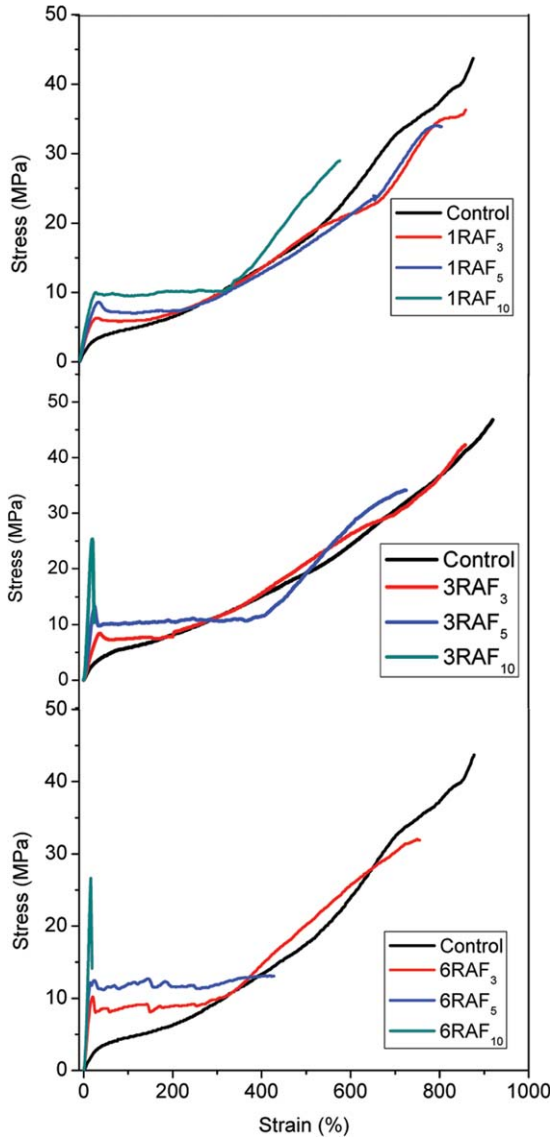

Figure 5. Engineering stress–strain behavior of TPU/short fiber composite as a function of fiber loading and length. [Color figure can be viewed in the online issue, which is available at wileyonlinelibrary.com.]

the TPU/aramid fiber composite as a function of fiber loading and length measured in the longitudinal direction (L) is represented in Figure 5. In contrast to the deformation behavior of the neat TPU, the short fiber reinforced TPU shows an inhomogeneous deformation behavior with different characteristic regions such as a well-defined linear elastic region, a yielding followed by a drop in stress (yield drop) and a stress plateau (irreversible plastic deformation) region. Yield strength is the stress at which a material begins to deform plastically. The knowledge of yield strength is very important in engineering structural design. Before the yield strength the material will deform elastically and will return to its original shape when the applied load is removed from it. But whenever the yield point is crossed some fraction of the deformation will be permanent and non-reversible. Table IV represents the yield strain, stress at yield point, and the yield plateau region of the aramid–TPU

Table IV. Yield Behavior of TPU/Short Fiber Composites with Various Fiber Length and Loading

Composite designation	Yield stress (MPa)	Yield strain (%)	Stress-plateau region (%)
$1RAF_3$	6.2 ± 0.9	40 ± 3	150 ± 5
$1RAF_5$	8.5 ± 1.2	38 ± 2	220 ± 8
$1RAF_{10}$	9.7 ± 2.1	36 ± 3.3	325 ± 12
$3RAF_3$	8.1 ± 1.1	34 ± 2	243 ± 8
$3RAF_5$	13.2 ± 1.7	25 ± 2.5	370 ± 14
$3RAF_{10}$	21.5 ± 2.8	24.8 ± 2.8	-
$6RAF_3$	10.28 ± 1.9	20.1 ± 1.5	262 ± 6
$6RAF_5$	12.4 ± 3.1	20.4 ± 2.8	426 ± 12
$6RAF_{10}$	26.6 ± 4.2	16.0 ± 3.2	-

composite as a function of fiber length and loading. It is clear from the table that the strain at which yielding starts decreases as the concentration as well as length of the short fiber increases. However, the yield stress gradually increases as the concentration and length of the fiber increases. The reinforcement of the amorphous phase (soft segment) by the short fiber causes an increase in the stress at the low strain region. The breaking or disturbances of the strain induced orientations of the soft segment by the presence of short aramid fiber may be responsible for the post-yield stress drop observed here with growing strain. The interface debonding between the fiber and the matrix may be also a probable reason for such kind of behavior. The sliding of fiber along the interface over a distance may be responsible for the irreversible plastic deformation after the yield strain is exceeded. In the plastic deformation region, the stress was found independent of strain and hence this region can be called a stress plateau region. The extent of stress plateau region highly depends on the short fiber length and loading. The very interesting observation is that after the yield or stress plateau region, the composite shows a sudden rise in stress with increase in the strain. This is usually referred to as the post-yield strain hardening effect.[26] This post-yield strain hardening may be due to the self-reinforcing of the composite owing to the reorientation of the short fibers in the direction of applied strain. The point at which the strain hardening starts after yielding is called the yield strain hardening transition. From Figure 5, it is also clear that the yield strain hardening transition increases as the length and loading of the short fiber increases. This can be thought that as the loading and length of the short fiber increases it takes more time to align the short fibers in the direction of applied strain due to more fiber entanglement. In the case of 1 mm short fiber filled system, the post-yield strain hardening was observed up to a loading of 10 phr short fiber. Whereas in the case of 3 mm short fiber–TPU composite, the post-yield strain hardening effect was observed up to 5 phr fiber loading. At 10 phr loading of short fiber, the composite shows failure immediately after the yield point without going for a stress plateau region. In the case of 6 mm short fiber filled TPU composite, the post-yield strain hardening was observed only up to 3 phr of short fiber loading. With 5 phr

Table V. The Mechanical Properties of the RFL Coated Short Aramid Fiber/TPU Composites as a Function of Fiber Length and Loading

Sample ID with mill direction		TS (MPa)	Elongation (%)	M at 10% (MPa)	M at 100% (MPa)	Young's modulus (MPa)	Hardness (Shore-D)
Control		43.7 ± 2.1	880 ± 21	1.4 ± 0.13	4.6 ± 0.22	22.4 ± 1.8	33 ± 1
$1RAF_3$	L	38.2 ± 1.5	856 ± 12	2.1 ± 0.09	5.5 ± 0.1	30.5 ± 2.1	34 ± 1
	T	38.8 ± 0.9	868 ± 14	2.2 ±0.1	5.2 ± 0.09	29.6 ± 1.8	
$1RAF_5$	L	34.9 ± 1.1	802 ± 21	2.4 ± 0.5	6.5 ± 0.82	48.4 ± 3.1	39 ± 1
	T	35.1 ± 1.2	815 ± 18	2.3 ± 0.3	5.8 ± 0.52	46.8 ± 2.8	
$1RAF_{10}$	L	30.5 ± 1.6	609 ± 31	3.5 ± 0.1	9.6 ± 0.17	69.8 ± 4.2	43 ± 2
	T	31.8 ± 1.8	597 ± 28	3.4 ± 0.2	9.4 ± 0.31	65.5 ± 2.8	
$3RAF_3$	L	36.3 ± 1.1	838 ± 24	2.4 ± 0.16	7.3 ± 0.17	35.5 ± 3.1	36 ± 1
	T	35.1 ± 1.2	840 ± 32	2.5 ± 0.18	7.6 ± 0.2	34.8 ± 2.9	
$3RAF_5$	L	32.5 ± 1.7	685 ± 35	4.9 ± 0.4	10.3 ± 0.13	58.7 ± 3.5	41 ± 1
	T	30.8 ± 1.5	679 ± 48	2.7 ± 0.3	9.3 ± 0.5	55.4 ± 2.5	
$3RAF_{10}$	L	22.5 ± 3.5	78 ± 16	7.8 ± 0.98	-	256.6 ± 19	46 ± 2
	T	16.5 ± 3.8	395 ± 19	5.1 ± 1.0	-	88 ± 14.6	
$6RAF_3$	L	30.3 ± 2.4	746 ± 85	6.2 ± 0.65	8.7 ± 0.08	101 ± 4.5	37 ± 1
	T	28.3 ± 2.6	762 ± 66	4.3 ± 0.82	8.4 ± 0.06	61.9 ±3.8	
$6RAF_5$	L	18.1 ± 9.5	541 ± 135	9.3 ± 1.2	11.5 ± 0.54	190 ± 6.5	41 ± 3
	T	17.3 ± 6.9	588 ± 95	6.8 ± 1.5	9.8 ± 1.2	63.9 ± 4.8	
$6RAF_{10}$	L	27 ± 3.2	45 ± 32	14.1 ± 1.7	-	501 ± 60	48 ± 3
	T	16 ± 2.8	92 ± 31	7.6 ± 1.3	-	174 ± 18.2	

L; Properties measured in the mill direction, T: Properties measured in the cross-mill direction.

loading, the composite shows failure after a yield plateau region up to a strain of 425%. Whereas at 10 phr loading a sudden failure occurs immediately after the yield point as observed in the case of 10 phr of 3 mm short fiber filled TPU composite. The inability to show post-yield strain hardening phenomenon in the case of 10 phr of 3 mm short fiber filled TPU and beyond 3 phr of 6 mm short fiber filled TPU may be due to restrictions of the fiber alignment by the fiber aggregation developed in the composite beyond the said loading of short fiber in the TPU matrix.

Tensile Properties: Effect of Fiber Orientation. The tensile properties such as the ultimate tensile strength, elongation at break (EB), Young's modulus (E-modulus), low strain modulus (10%), and high strain modulus (100%) as a function of short fiber length and loading measured in the mill direction (L) and cross-mill direction (T) of the molded composite is shown in the Table V. The addition of short fibers dramatically increases the elastic modulus as a function of fiber loading and length. This may be due to polar interactions between the RFL coated aramid fiber and the matrix as well as a kind of mechanical bonding between the fibrillated aramid fiber and the TPU matrix. More details about the fibrillation have been explained in the next sections. The better retention in the fiber length even after intensive shear mixing could be also a probable reason for the observed hike in the E-modulus with the fiber length and loading. A clear anisotropic behavior particularly in Young's modulus and 10% modulus values have been observed in the mill and cross-mill direction due to fiber orientation. The modulus observed in the mill direction was always higher than that observed in the cross mill direction due to the presence of more oriented fibers in the direction of applied tensile force. Similar phenomena were also previously noticed by many researchers.[7] It is clear from the Table V that the ultimate tensile strength and elongation at break decreases sharply with increasing fiber length and loading. In Figure 4, pristine TPU always shows high strength and elongation at break owing to the orientations of its soft and hard segment in the direction of applied strain or otherwise called strain induced crystallization. The incorporation of short fibers may disturb the smooth orientations of the soft and hard segments of the TPU. This in-homogeneity in the behavior of soft and hard segment orientation to the tensile deformation reduces the breaking strain and hence the ultimate tensile strength. As the concentration as well as length of the short fiber increases it may severely prohibit the orientations of the soft and hard domains due to the formation of aggregated fiber lumps and thereby drastically reduces elongation at break and hence the tensile strength. However, the Young's modulus, the low strain modulus and hardness were found to increase with fiber loading and length may be due to the soft segment reinforcement by the short aramid fiber. As observed in the case of E-modulus, the tensile strength measured in the longitudinal direction (mill direction) was higher than those measured in the transverse direction (cross-mill direction). However, the effect was very much pronounced with high fiber volume fraction (10 phr) with a short fiber length of 3 and 6 mm.

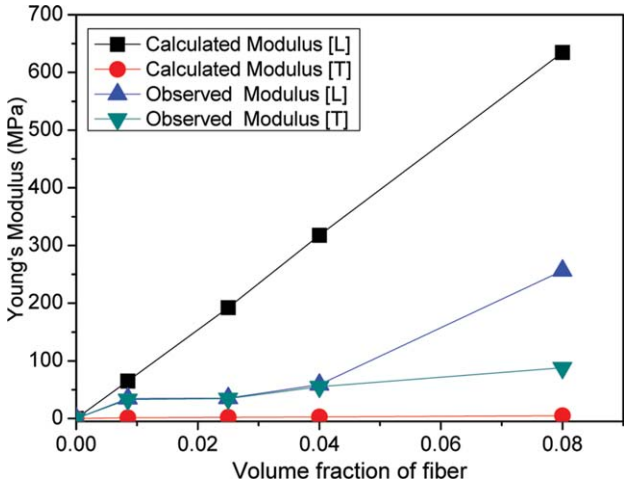

Figure 6. Young's modulus of 3 mm short fiber/TPU composite measured in the longitudinal (L) and transverse (T) direction as a function of volume fraction of fiber. [Color figure can be viewed in the online issue, which is available at wileyonlinelibrary.com.]

Theoretical Modeling of Young's Modulus. The E-modulus depends strongly to the fiber orientation and is not very sensitive to the fiber–matrix interface adhesion. Hence the variation of E-modulus measured in different directions can be used as a tool to determine the anisotropy in short fiber orientation. In this system, we made an attempt to predict the anisotropy in Young's modulus due to variations in fiber orientations on a 3 mm short fiber reinforced TPU composite with the help of a well known Halpin–Tsai model. According to this model, the longitudinal (E_L) and the transverse (E_T) Young's modulus of the composite can be calculated using the following equations:

$$E_L = \frac{1+2\,(l_f/d_f)\eta_L V_f}{1-\eta_L V_f} E_m \tag{1}$$

$$E_T = \frac{1+2\,\eta_T V_f}{1-\eta_T V_f} E_m \tag{2}$$

where η_L and η_T are given by:

$$\eta_L = \frac{\left(\frac{E_f}{E_m}\right)-1}{\left(\frac{E_f}{E_m}\right)+2\left(\frac{l_f}{d_f}\right)} \tag{3}$$

$$\eta_T = \frac{\left(\frac{E_f}{E_m}\right)-1}{\left(\frac{E_f}{E_m}\right)+2} \tag{4}$$

where η_L and η_T are the Young's modulus of the composite in the longitudinal and transverse directions, respectively. E_m, Young's modulus of the pristine TPU matrix; E_f, Young's modulus of the fiber; l_f, length of the fiber; d_f, diameter of the fiber, and V_f is the volume fraction of the fibers in the composites. The Young's modulus values calculated using the above Halpin–Tsai equations and the experimentally obtained Young's modulus are shown in Figure 6. It is seen from the figure that both the longitudinal and transverse Young's modulus were almost similar up to a fiber loading of 5 phr. This explains a great randomization in the fiber orientation distribution during the compression molding. As the volume fraction of fiber increases (as in the case with 10 phr fiber filled TPU composite), the randomization in fiber orientations from the longitudinally aligned structure is minimized due to restricted movement of the short fiber during compression molding. As a result, a significant difference has been observed in the longitudinal as well as transverse E-modulus values at 10 phr short fiber loading. It is also important to note from the graph that the observed modulus in the longitudinal direction is less than the calculated E- modulus values at all fiber loading. Whereas, the observed E- modulus values in the transverse direction are always higher than the calculated one. This opposite trend in deviation between the calculated and the observed modulus in case of longitudinally and transversely oriented fibers is also supporting some randomness in fiber orientation during molding of the composite.

Effect of PB-g-MA as a Dispersing Agent. A very good dispersion of short fibers into the polymer matrix is one of the primary requirements for developing any high performance short fiber composite. It has been already observed that the aggregation tendency for polar fibers like aramid is more during fiber mixing due to inter H-bonding. This would create severe fiber aggregation especially at high fiber loading. However, it is very much essential to incorporate sufficient amount of high length fibers on to the polymer matrix to achieve better mechanical properties. In this system, a severe dispersion problem at 10 phr of 3 mm short fiber and beyond 5 phr of 6 mm short aramid fiber in the TPU matrix. This fiber dispersion problem drastically reduces the mechanical properties such as tensile strength and elongation at break with increased volume fraction of fillers. The toughness of the composite also gets reduced as the concentration as well as the length of the short fiber increases.

In order to understand the distribution and the state of short fiber after the process of mixing and molding, we have analyzed the tensile fractured surface morphologies of the composite using scanning electron microscopy under different magnification. Figure 7(a–c) represents the tensile fractured surface morphologies of a 10 phr fiber filled TPU composites having different fiber length such as 1, 3, and 6 mm, respectively, with magnifications of 100× and 500×. It is very clear from the Figure 7(a) that in 1 mm short fiber filled TPU even at a loading of 10 phr, the short fibers were distributed evenly throughout the matrix. However, the tensile fractured surfaces of 3 mm as well as 6 mm of 10 phr fiber filled composite exhibits severe fiber entanglement and aggregation. Also it is worth noting from the Figure 7(b,c) that some fibers affected by fibrillation, the longitudinal splitting of larger diameter fibers into thinner fibrils.[27] On the other hand, from the morphological analyses of a 5 phr of 3 mm fiber filled composite, we exposed to view that the intensity of fibrillation was not much pronounced. However, it was still pronounced even at 5 phr of 6 mm short fiber composite. From these detailed morphological analyses, it can be arrived that the intensity of fibrillation highly depends on the length and volume fraction of short fibers in the composite. This is because, as the length and loading of short fiber increases, the mechanical abrasion of larger diameter fibers may be more due to the increased shear deformation during mixing.

Applied Polymer SCIENCE

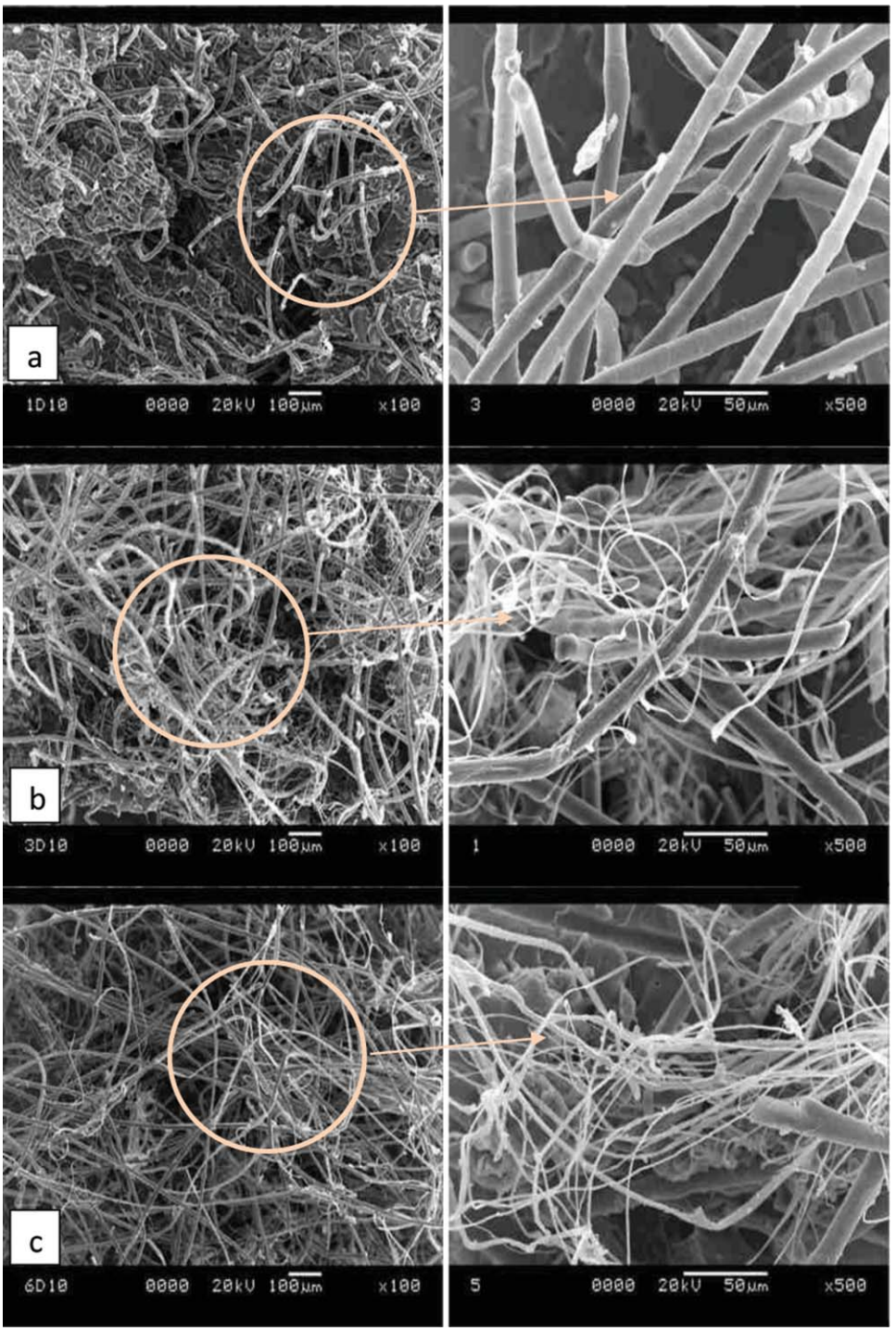

Figure 7. SEM photomicrographs of tensile fractured surfaces of 10 phr short fiber filled composites having various fiber length (a) $1RAF_{10}$ (b) $3RAF_{10}$ (c) $6RAF_{10}$ with magnification of 100× (left) and 500× (right). [Color figure can be viewed in the online issue, which is available at wileyonlinelibrary.com.]

Figure 8 shows a fibrillated single fiber having fibril diameters approximately 1 to 2 μ as compared to the unfibrillated fiber with an original diameter of 12 μ. Also, it is very clear from the figure that due to fibrillation, some shallow grooves are created on the fiber surface in the longitudinal direction. Whereas the unfibrillated fiber surface was very smooth and is totally free from any such deep grooves. Earlier many researchers have claimed that fibrillation impart several benefits to a reinforcing fiber.[28] In this system, a synchronous advantages and disadvantages due to fibrillation have been noticed. For instance, the tremendous increase in the stiffness (E-modulus) as well as low strain modulus (10% modulus) with short fiber loading and

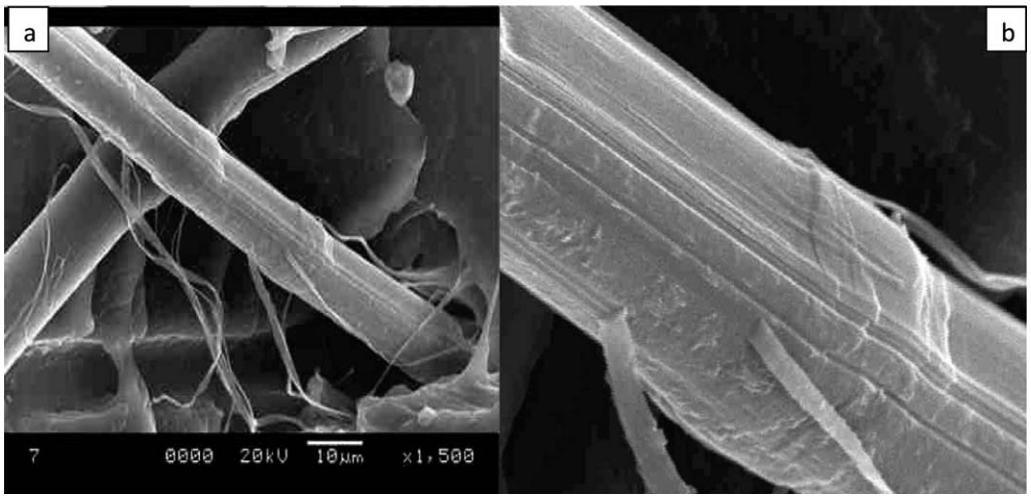

Figure 8. SEM photomicrograph of a fibrillated single fiber with an enlarged view on the right side.

length could be one of the advantages due to fibrillation. It is quite clear from Figure 7(b,c) that fibrillation increases surface area of a perfectly cylindrical unfibrillated fiber. This enhanced surface area of the fibrillated fiber can increase the mechanical bonding with the surrounding matrix. Moreover, the shallow grooves generated on the fiber surface due to fibrillation, as shown in Figure 8, would also provide more contact points, which further enhance the degree of mechanical interlocking between the fibrillated fiber and the TPU matrix. From another point of view, the fibrils which are generated from the larger fiber can act as hooks or fasteners to intertwine its adjacent fibers, thereby creating aggregate lumps during mixing. This aggregated fiber lumps creates imperfections such as surface flaws on the composite which act as a failure point to an applied load causing an early failure (low EB) and low tensile strength especially in composite with high fiber length and loading. Therefore, it is very much essential to control or reduce the degree of fibrillation. In order to control the degree of fibrillation and hence to achieve a good quality of fiber dispersion on to the TPU matrix, we have applied an instant coating of PB-*g*-MA on to the surface of aramid fiber prior to mixing it with the TPU matrix. The details of the procedure adopted for the coating and the chemical modification involved between RFL coated aramid fiber and PB-*g*-MA are clearly mentioned in our previous article.[29] As per the same procedure adopted in our earlier work, we have treated the RFL coated aramid short fiber with PB-*g*-MA in different concentration and mixes with TPU as per the mixing schedule mentioned in the "Experimental" section.

Figure 9 and Table VI represents the stress–strain behavior and the corresponding tensile properties of a 10 phr of 3 mm short aramid fiber treated with different concentrations of PB-*g*-MA reinforced TPU. It is clear from the figure that 10 phr fiber filled TPU composite shows a sudden failure immediately after yielding. However, the composite developed after pre-treating the fiber with 3 phr of PB-*g*-MA exhibit a tough deformation behavior with a prominent irreversible plastic deformation region up to a strain of 500% after the yield and yield drop phenomenon. This means that addition of only 3 phr of PB-*g*-MA increases the failure strain (EB) of a 10 phr fiber filled TPU composite by 840%. Upon adding 5 phr of PB-*g*-MA, the behavior of stress–strain curve was almost similar to that of 3 phr of PB-*g*-MA treated fiber filled TPU composite with an additional post-yield strain hardening effect beyond a strain of 500%. This means that with the treatment of 5 of phr PB-*g*-MA, the fibers in the composite are able to orient in the direction of the applied strain after the irreversible plastic deformation. As the concentration of PB-*g*-MA increases to 10 phr, the composite exhibits a homogeneous deformation behavior with no yielding or yield drop phenomena. In this case, the composite shows the highest tensile strength and the highest elongation at break. The toughness of the composite also increases which is very clear from the area under the stress–strain curve as

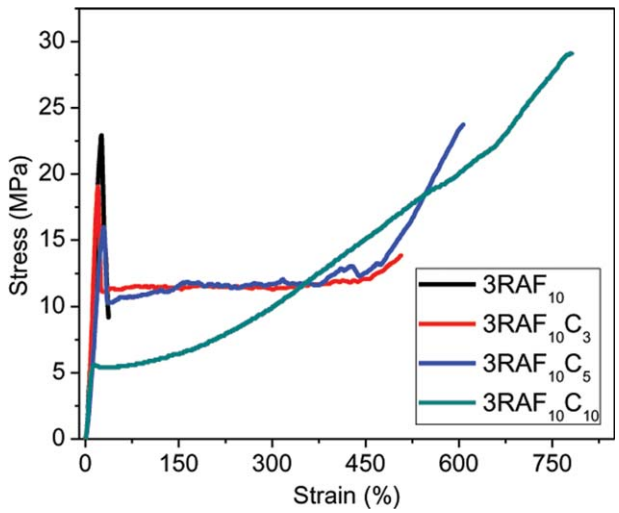

Figure 9. Engineering stress-strain curves of 10 phr of 3 mm short fiber loaded composite ($3RAF_{10}$) with various concentrations of PB-*g*-MA. [Color figure can be viewed in the online issue, which is available at wileyonlinelibrary.com.]

Table VI. Mechanical Properties of 10 phr of 3 mm Short Fiber Loaded Composites Pre-treated with Different Concentrations of PB-*g*-MA

Sample ID	$3RAF_{10}$ C_3		$3RAF_{10}$ C_5		$3RAF_{10}$ C_{10}	
Orientation	L	T	L	T	L	T
TS (MPa)	23 ± 3.2	14 ± 2.8	25 ± 2.6	18 ± 2.2	29.5 ± 2.9	22.5 ± 3.2
EB (%)	470 ± 15	525 ± 12	535 ± 16	565 ± 14	622 ± 24	702 ± 21
M at 10% (MPa)	7.2 ± 1.0	3.7 ± 0.9	8.2 ± 1.2	3.78 ± 1.0	4.34 ± 0.8	4.37 ± 0.7
M at 100% (MPa)	11.5 ± 1.8	10.4 ± 1.6	10.7 ± 1.4	9.1 ± 1.2	6.86 ± 0.9	6.5 ± 0.7
E-Modulus (MPa)	248 ± 18	78 ± 13.8	251 ± 16	72 ± 14	247 ± 15	63 ± 11

L; Properties measured in the mill direction, T: Properties measured in the cross-mill direction.

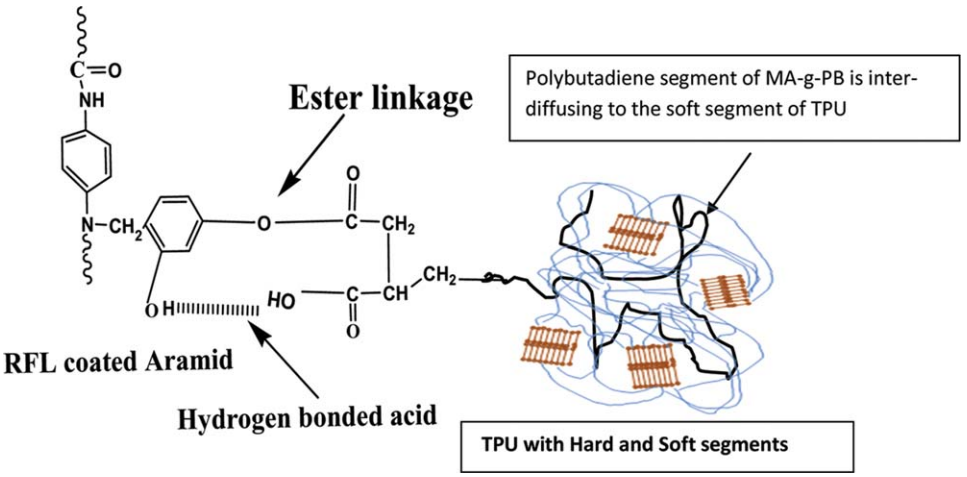

Figure 10. Plausible interaction mechanism of PB-*g*-MA treated RFL coated aramid short fiber with TPU matrix. [Color figure can be viewed in the online issue, which is available at wileyonlinelibrary.com.]

represented in Figure 9. However, the low strain modulus (10% modulus) of the composite is reduced at this level of PB-*g*-MA. This enhancement in the tensile properties of the composites indicate that low molecular weight PB-*g*-MA acts as a coupling agent for the RFL coated aramid short fiber–TPU matrix and thereby increase the adhesion between the fiber and the TPU matrix. From our previous studies, it has been observed that during pre-treatment, anhydride part of PB-*g*-MA gets attached to the RFL coated aramid fiber through ester linkage.[30] Hence it is reasonable to believe that the butadiene segment (nonpolar part) of PB-*g*-MA diffuses into the soft segment (which is mostly nonpolar hydrocarbon) of the TPU and forms interchain entanglement during mixing, thereby improving the adhesion between the short aramid fiber and the TPU matrix. As a result, the transfer of stress from the matrix to fiber has been improved, which leads to higher tensile strength. Figure 10 represents one of the possible interaction mechanism between PB-*g*-MA treated RFL coated aramid short fiber and the TPU matrix. In addition to the tensile property improvements, the PB-*g*-MA treated short fiber shows excellent quality of fiber dispersion in the TPU matrix. The dispersion of 6 mm short fiber into the TPU matrix beyond a concentration level of 5 phr was found to be very difficult due to severe fibrillation and the subsequent fiber aggregation. However, a 5 phr PB-*g*-MA treated 6 mm short fiber even at a loading of 10 phr shows excellent fiber dispersion. Moreover, its stress–strain behavior, as shown in Figure 11, exhibits a tough plastic deformation up to a strain of 370%. This indicates that PB-*g*-MA also serves as an impact modifier to dissipate more amount of energy before the failure

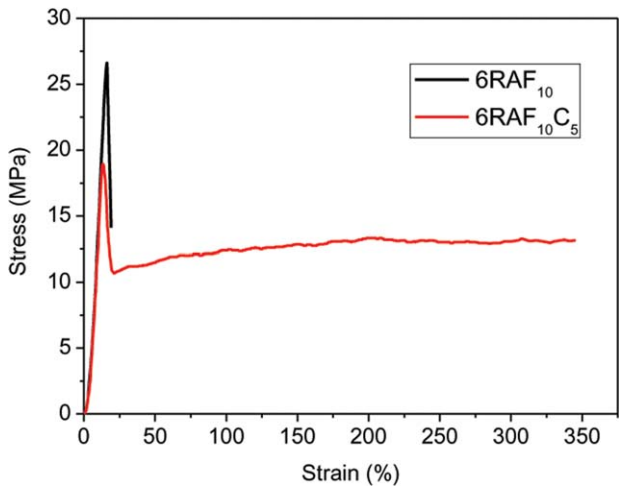

Figure 11. Stress–strain behavior of 10 phr of 6 mm short fiber loaded composite ($6RAF_{10}$) and that treated with 5 phr PB-*g*-MA ($6RAF_{10}C_5$). [Color figure can be viewed in the online issue, which is available at wileyonlinelibrary.com.]

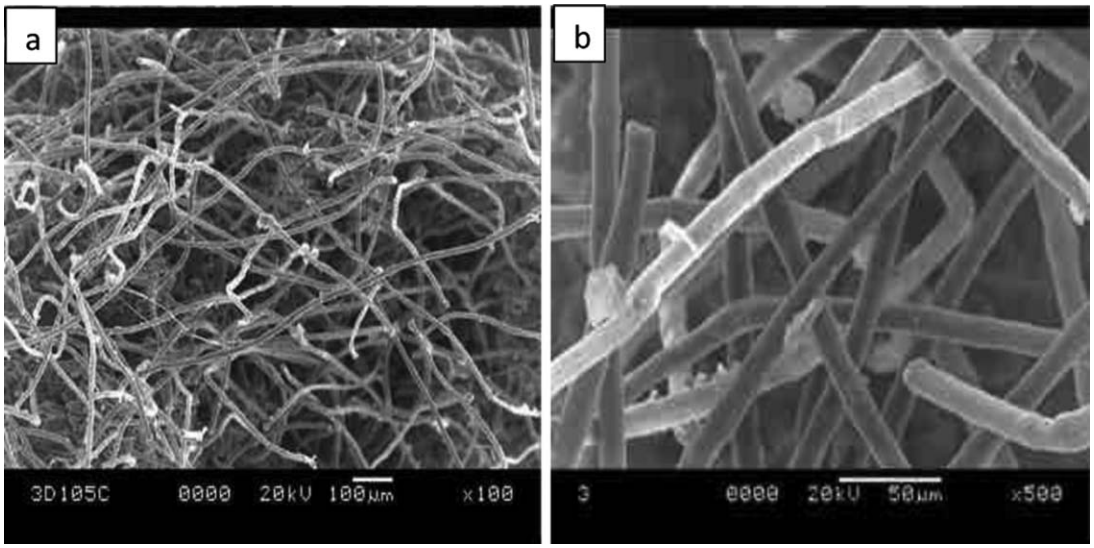

Figure 12. SEM photomicrographs of tensile fractured surfaces of the composite $3RAF_{10}C_5$ under different magnifications.

occurs. A detailed morphological analysis on the tensile fractured surfaces of a PB-*g*-MA treated short aramid fiber reinforced TPU composite were carried out to get a better insight to understand how PB-*g*-MA treatment enhances the fiber dispersion on to the TPU matrix. Figure 12(a,b) represents the tensile fractured surface morphologies of a 10 phr of 3 mm short fiber pre-treated with 5 phr PB-*g*-MA filled TPU matrix under various magnifications. It is clear from the figures that after the pre-treatment with PB-*g*-MA, the fibers are uniformly distributed in the matrix without any severe fiber aggregation. Moreover, the fibrillation was totally absent or reduced to a great level due to the effect of this pre-treatment. It is believed that PB-*g*-MA, which is chemically coated over the fiber surface acts as a lubricant between the stiff aramid fibers during shear mixing, thereby reducing the amount of fibrillation which is responsible for the severe fiber aggregation observed in this system. SEM analyses were also carried out at the fiber matrix interface. Figure 13(a,b) represents the tensile fractured surfaces of the composite at the interface region without any PB-*g*-MA treatment and with 5 phr of PB-*g*-MA, respectively. As we have already discussed that the fibers without any PB-*g*-MA coating is interacted with the TPU matrix via polar interactions and mechanical bonding with the rough fibrillated fiber surface. Because of these two combined physical interacting effect, it can withstand more tensile stress at the low strain region. As the strain increases, it may get de-bonded from the matrix leaving irregular surfaces on the matrix at the interface region. The surface irregularities generated on the matrix due to fiber de-bonding can also be seen in Figure 8. These irregularities generated on the surfaces of the TPU matrix after the de-bonding of the

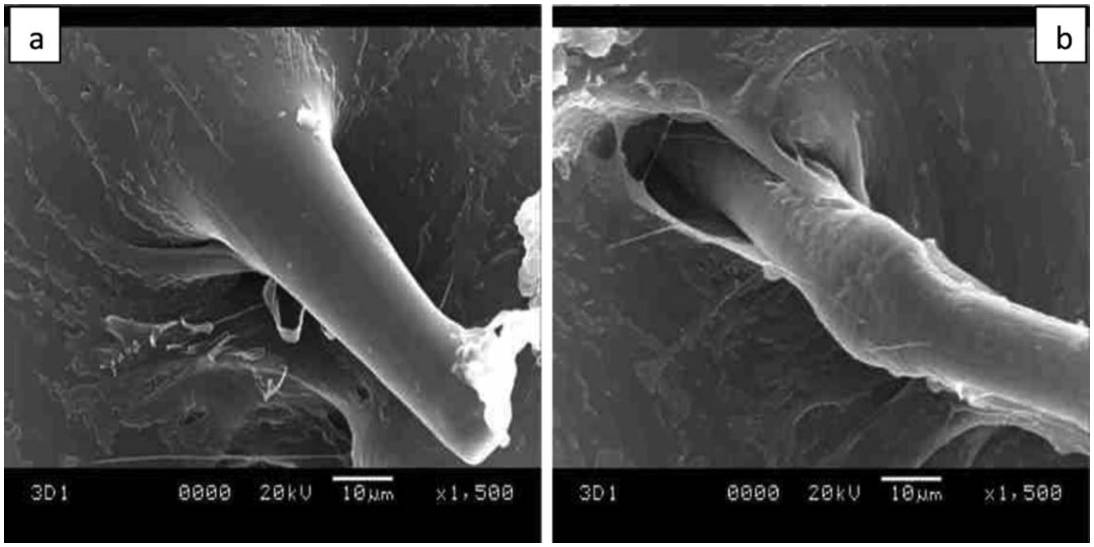

Figure 13. SEM photomicrographs of tensile fractured surfaces of the composite at the interface regions (a) $3RAF_{10}$ and (b) $3RAF_{10}$ C_5.

short fiber is a strong evidence of the mechanical anchoring or mechanical bonding between the fiber and the matrix. On the other hand, the PB-*g*-MA coated aramid fiber reinforced TPU composite created a ductile interface between the polymer and the fiber as shown in Figure 12(b). It is evident from the figure that the fibers appear to have been extensively stretched at the interface along with the matrix. The generation of such ductile interface may be one of the reasons for an extensive plastic deformation (tough deformation behavior) that we have observed in the stress–strain curves of PB-*g*-MA treated fiber composite. Since the coating greatly reduces the degree of fibrillation, the chances of more mechanical interlocking (mechanical anchoring) between the fiber and the matrix also reduces. This may be a reason for the drop in stress at the low deformation.

CONCLUSIONS

This study is primarily aimed at an analysis of a low molecular weight maleic anhydride grafted polybutadiene as a dispersing agent for short aramid fiber in thermoplastic polyurethane. A straight forward and economic method of treatment has been adopted for coating PB-*g*-MA on the surface of the aramid fiber prior to mixing it with TPU matrix. It has been observed from the SEM analyses that the fibrillation of the aramid fiber during melt mixing causes a severe fiber dispersion problem, which reduces the ultimate tensile strength and the elongation at break especially with 3 and 6 mm short fiber at 10 phr of fiber loading. The low molecular weight PB-*g*-MA used in this study is found to be a good choice for controlling the fibrillation and thereby increase the quality of fiber dispersion in the TPU matrix. The tensile strength, elongation at break, and a favorable stiffness and toughness balance of the composite along with a high quality of fiber dispersion even with 6 mm short fiber at 10 phr loading could be achieved with the use of 5 phr PB-*g*-MA.

ACKNOWLEDGMENT

The authors are thankful to Teijin Aramid BV, The Netherlands for providing the Technora short fibers.

REFERENCES

1. De, S. K.; White, J. R. Short Fiber Polymer Composites; Woodhead: England, **1996**.
2. Folkes, M. J. Short Fiber Reinforced Thermoplastics; Wiley: New York, **1982**.
3. Derringer, D. C. *J. Elastoplast.* **1971**, *3*, 230.
4. Goettler, L. A.; Leib, R. I.; Lambright, A. J. Technical Paper; American Chemical Society, Atlanta, **1979**; p 27.
5. Jassal, M.; Ghosh, S. *Indian J. Fibre Textile Res.* **2002**, *27*, 290.
6. Arroyo, M.; Bell, M. *J. Appl. Polym. Sci.* **2002**, *83*, 2474.
7. Kutty, S. K. N.; Nando, G. B. *J. Appl. Polym. Sci.* **1991**, *43*, 1913.
8. Kutty, S. K. N.; Nando, G. B. *J. Appl. Polym. Sci.* **1992**, *46*, 471.
9. Kutty, S. K. N.; Nando, G. B. *Polym. Degrad. Stab.* **1992**, *38*, 187.
10. Correa, R. A.; Nunes, R. C. R. *Polym. Compos.* **1998**, *19*, 152.
11. Correa, R. A.; Nunes, R. C. R.; Lourenco, V. L. *Polym. Degrad. Stab.* **1996**, *52*, 245.
12. Prasithphol, W.; Young. R. J. *J. Mater. Sci.* **2005**, *40*, 5381.
13. Vajrasthira, C.; Amornsakchai. T.; Limcharoen, S. B. *J. Appl. Polym. Sci.* **2003**, *87*, 1059.
14. Chantaratcharoen, A.; Sirisinha, C., Amornsakchai, T.; Limcharoen, S. B.; Meesiri, W. *J. Appl. Polym. Sci.* **1999**, *74*, 2414.
15. Tarantili, P. A.; Andreopoulos, A. G. *J. Appl. Polym. Sci.* **1999**, *65*, 267.
16. Liu, T. M.; Zheng, Y. S.; Hu, J. *Polym. Bull.* **2011**, *66*, 259.
17. Wu, S. R.; Sheu, G. S.; Shyu, S. S. *J. Appl. Polym. Sci.* **1996**, *62*, 1347.
18. Mori, M.; Uyama, Y.; Ikada, Y. *Polymer* **1994**, *34*, 5336.
19. Andreopoulos, A. G. *J. Appl. Polym. Sci.* **1989**, *38*, 1053.
20. Amornsakchai, T.; Sinpatanapan, B.; Limcharoen, S. B.; Meesiri, W. *Polymer* **1999**, *40*, 2993.
21. Ahamad, I.; Chin, T. S.; Cheong, C. K.; Jalar, A.; Abdullah, I. *Am. J. Appl. Sci.* **2005**, 14.
22. Akhtar, S.; De, P., De, S. K. *J. Appl. Polym. Sci.* **1986**, *32*, 5123.
23. Akbarian, M.; Hassanzadeh, S.; Moghri, M. *Polym. Adv. Technol.* **2008**, *19*, 1894.
24. Szycher, M. Szycher's Handbook of Polyurethane; CRC Press: London, **1999**.
25. Hammond, P. T.; Nallicheri, R. A.; Rubner, M. F. *Mater. Sci. Eng. A.* **1990**, *126*, 281.
26. Bicerano, J. Prediction of Polymer Properties. Marcel Dekker, Inc.: New York, **2002**.
27. Hashimoto, A.; Satoh, M.; Iwasaki, T.; Morita, M. *J. Mater. Sci.* **2002**, *37*, 4013.
28. Arthur, R. H.; Phillip, B. F. *J. Mater. Sci.* **1990**, *25*, 3659.
29. Shibulal, G. S.; Naskar, K. *J. Polym. Res.* **2011**, *18*, 2295.
30. Shibulal, G. S.; Naskar, K. *Exp. Polym. Lett.* **2012**, *6*, 329.